Polymer Encapsulation of Fine Particles by a Supercritical Antisolvent Process

Yulu Wang, Robert Pfeffer, and Rajesh Dave
New Jersey Center for Engineered Particulates, New Jersey Institute of Technology, Newark, NJ 07102

Robert Enick
Dept. of Chemical Engineering, University of Pittsburgh, Pittsburgh, PA 15206

DOI 10.1002/aic.10323
Published online in Wiley InterScience (www.interscience.wiley.com).

Coating and encapsulation of fine particles with polymer using a supercritical antisolvent (SAS) coating process was investigated in this research. Synthesized submicron silica particles were used as host particles and poly(lactide-co-glycolide) (PLGA), a biodegradable polymer used for controlled release of drugs, was chosen as the coating material. In the SAS coating process a suspension of silica particles in an acetone–polymer solution was sprayed through a capillary nozzle into supercritical (SC) CO_2, which acts as an antisolvent for the acetone. A rapid mutual diffusion between the SC CO_2 and the acetone causes supersaturation of the polymer solution, leading to nucleation and precipitation of the polymer to encapsulate the silica particles. The operating parameters that have an effect on the coating process, such as polymer to particle weight ratio, polymer concentration, temperature, pressure, flow rate of polymer solution, and the addition of a SC CO_2 soluble surfactant, were systematically studied. It is shown that the polymer to silica ratio and the polymer concentration are critical for the successful encapsulation of silica particles with minimum agglomeration. © 2005 American Institute of Chemical Engineers *AIChE J,* 51: 440–455, 2005

Keywords: encapsulation, coating, agglomeration, particle, supercritical CO_2

Introduction

Coating or encapsulation of fine particles to produce tailored surface properties is of great interest in the pharmaceutical, cosmetic, food, and agrochemical industries. The particle surface can be engineered to specific physical, chemical, and biochemical properties by spreading a thin film of material on the surface of the particles. Consequently, the flowability, dissolution rate, dispersability, chemical reactivity, bioefficacy, and hydrophilicity of particles can be modified for a variety of applications.[1-3]

Conventional techniques for the encapsulation of fine particles, such as emulsion evaporation, phase separation, spray-drying, freeze-drying, and so forth, require large amounts of organic solvents, surfactants, and other additives, leading to volatile organic compound (VOC) emissions and other waste streams. Other drawbacks include low encapsulation efficiency and further processing of the products such as downstream drying, milling, and sieving, which are usually necessary. In addition, residual toxic solvent in the end products, temperature and pH requirements, and strong shear forces are daunting challenges for maintaining the fragile protein structure in the encapsulation of pharmaceutical ingredients.

During the past decade, supercritical fluid processes such as RESS (rapid expansion of supercritical solutions), SAS (supercritical antisolvent), and GAS (gas antisolvent) have attracted increasing attention for particle engineering, including fine particle formation, coating, and encapsulation. Supercritical

Correspondence concerning this article should be addressed to R. Pfeffer at pfeffer@adm.njit.edu.

carbon dioxide (SC CO_2), in particular, is an ideal processing medium for particle encapsulation because of its relatively mild critical conditions (T_c = 304.1 K, P_c = 7.38 MPa). Furthermore, SC CO_2 is nontoxic, nonflammable, relatively inexpensive, readily available, and chemically stable.

A number of SC processes for the encapsulation of particles with polymer or composite particle formation for the controlled release of drugs have been reported. Tom and Debenedetti[4] studied the coprecipitation of poly(L-lactide) (PLA)–pyrene composite particles by a RESS process. In their research, PLA and pyrene were extracted by SC CO_2 in two separate extraction columns. The two supercritical solutions were subsequently co-introduced through a nozzle into a precipitation vessel. A sudden depressurization results in the loss of solvent strength of the SC CO_2, leading to a high degree of supersaturation of the solute and the formation of composite particles of pyrene distributed in a polymer matrix of PLA. Similar research involving the microencapsulation of naproxen with polymer using RESS was done by Kim et al.[5] Mishima et al.[6] reported the microencapsulation of proteins with poly(ethylene glycol) (PEG) by RESS. Ethanol (about 38.5 wt %) was used as a cosolvent to enhance the solubility of PEG in SC CO_2. The results indicated that core particles of lipase and lysozyme were completely encapsulated by PEG without agglomeration.

Recently, Wang et al.[7] used a modified RESS process of extraction and precipitation to coat particles with polymer. The coating polymer and particles to be coated (host particles) were placed in two different high-pressure vessels, respectively. The coating polymer was first extracted by SC CO_2. The resulting supercritical polymer solution was then introduced into the host particle vessel. By adjusting the temperature and pressure, the polymer solubility in SC CO_2 was lowered and nucleation and precipitation of polymer took place on the surface of the host particles and a fairly uniform polymer coating was formed. However, the potential application of RESS for particle coating or encapsulation is limited because the solubility of polymers in SC CO_2 is generally very poor.[8]

Pessey et al.[9,10] demonstrated the deposition of copper on nickel particles and of copper on permanent magnetic $SmCo_5$ particles by the thermal decomposition of an organic precursor of bis(hexafluoroacetylacetonate)copper(II) in a supercritical fluid. They produced a core–shell structure of copper on the surface of core (host) particles in SC CO_2 under conditions of temperature up to 200°C and pressure up to 190 bars. Clearly this encapsulation method is not attractive to the pharmaceutical industry interested in coating drug powders because the high temperature required will be harmful for most drug powders.

Compared to RESS, the SAS process offers much more flexibility in terms of choosing suitable solvents. Furthermore, SAS has advantages over RESS because SAS is usually operated under mild conditions compared with those of RESS, which is associated with relatively high temperature and high pressure.[11-13] Therefore RESS is also less attractive from the perspectives of safety and cost.

In SAS, SC CO_2 is used as an antisolvent (instead of a solvent as in RESS) to extract an organic solvent from a solution containing the solute, which is desired as the coating or encapsulation material. The solution is in the form of tiny droplets, produced by a nozzle through which the solution is sprayed into a high-pressure vessel. When the droplets contact the SC CO_2, very rapid diffusion between the droplets and the SC CO_2 takes place, inducing phase separation and precipitation of the solute. SAS offers the capability of producing free-flowing particles in a single step at moderate pressure and temperature.

Young et al.[14] studied the encapsulation of lysozyme with a biodegradable polymer by precipitation with a vapor-over-liquid antisolvent (below supercritical conditions), which is a modified SAS process. Encapsulation of 1- to 10-micron lysozyme particles was achieved in PLGA microspheres without agglomeration. More recently, our research group applied the SAS process for the encapsulation of nanoparticles with Eudragit.[15] A suspension of silica nanoparticles in a polymer solution was sprayed into SC CO_2 through a capillary tube. The subsequent mutual diffusion between SC CO_2 and polymer solution droplets resulted in a high degree of supersaturation, causing a heterogeneous polymer nucleation induced by the phase transition, with the silica nanoparticles acting as nuclei. Thus the nanoparticles were individually encapsulated in polymer with very little agglomeration.

In our previous work,[15] the amount of polymer used was found to affect both the coating thickness and the degree of agglomeration. The objective of this study is to thoroughly investigate the effects of various process parameters, such as the polymer weight fraction, polymer concentration, temperature, pressure, and flow rate, on the coating of particles and the agglomeration of the coated particles in the SAS coating process. Some CO_2-soluble surfactants will also be applied to determine whether they help minimize agglomeration. We will also attempt to propose a mechanism for the SAS coating process based on our experimental results.

Experimental

Materials

The host particles that were used in our SAS coating study were spherical silica particles (size ~ 0.5 μm), which were synthesized in our laboratory using the classic Stöber process.[16] Tetraethyl orthosilicate (TEOS; MW 208, 98%) was purchased from Sigma-Aldrich Co. (St. Louis, MO). Ammonium hydroxide (28.87%) was purchased from Fisher Scientific (Pittsburgh, PA) and anhydrous ethyl alcohol from AAPER Alcohol (Shelbyville, KY). The chemicals were used without further treatment.

The coating material was poly(lactide-*co*-glycolide) (PLGA; Resomer® 502, MW 12,000, 50/50, T_g 40–55°C), supplied from Boehringer Ingelheim Chemicals, Inc. (Petersburg, VA). Acetone was purchased from Aldrich (Milwaukee, WI) and used as received. Liquid CO_2 was obtained from the Matheson Company (Parsippany, NJ). Surfactants of random poly(fluoroalkylacrylate-*co*-styrene) (PFS; 29 mol % styrene) and poly(fluoroalkylacrylate) homopolymer (PFA) were synthesized in Professor Robert Enick's laboratory at the University of Pittsburgh. The surfactant Krytox 157 FSL, a perfluoropolyether terminated with a carboxylic acid at one end, was supplied by DuPont Chemicals (Deepwater, NJ). These surfactants as shown in Table 1 were used as received without further treatment. The chemical structures of the coating polymer and the surfactants are given in Figure 1.

Table 1. Polymer and Polymeric Surfactant Properties

Polymer	State	Commercial Name	Molecular Weight	Content (% molar)
PLGA	Solid	Resomer® 502 (RG 502)	12,000	50% polyglycolide
PFS	Solid	N/A	539,600	29% polystyrene
PFA	Solid	N/A	86,200	100%
PFPE	Liquid	Krytox® 157 FSL	2,500	100%

Methods

In the preparation of spherical silica particles, pure alcohol, ammonium hydroxide, and deionized water were mixed in an Erlenmeyer flask at predetermined concentrations. TEOS was then added to the mixture that was stirred by a magnetic bar. TEOS underwent hydrolysis in water and grew into spherical silica particles, with ammonia acting as a morphological catalyst. After 24 h of reaction, the solution turned into a milky suspension. The resulting suspension was centrifuged at 3000 rpm for 5 min. The supernatant liquid was then drained and the particulate sediment was redispersed in pure alcohol. This washing step was needed for the removal of unreacted TEOS and water, and was repeated twice. Finally, the sediment of silica particles was redispersed in acetone to produce a suspension for further use in the SAS coating experiment.

Figure 2 shows a schematic diagram of the experimental apparatus, which consists of three major components: a suspension delivery system, a CO_2 supply system, and a stainless steel precipitation chamber equipped with a pressure gauge (Parr Instruments, Moline, IL). The precipitation chamber has a volume of

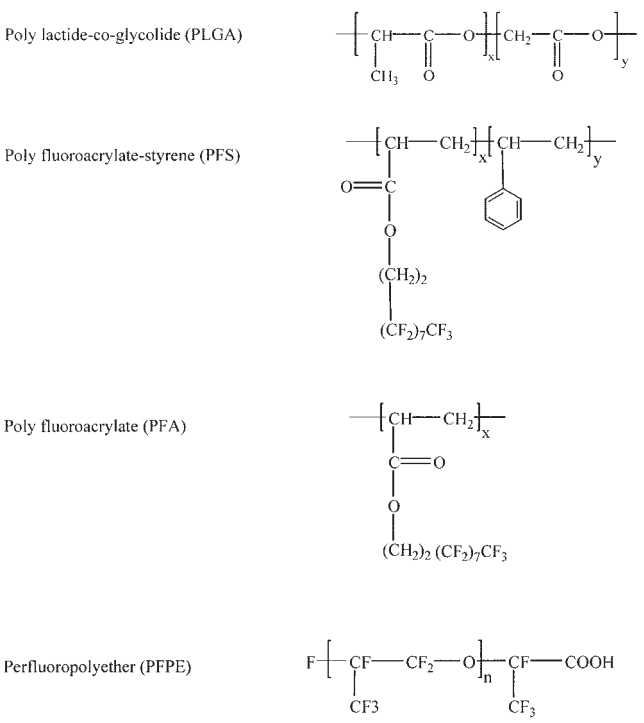

Figure 1. Repeat unit structure of poly(lactide-*co*-glycolide) (PLGA), polyfluoroacrylate–styrene (PFS), polyfluoroacrylate (PFA), and perfluoropolyether (PFPE) used in this study.

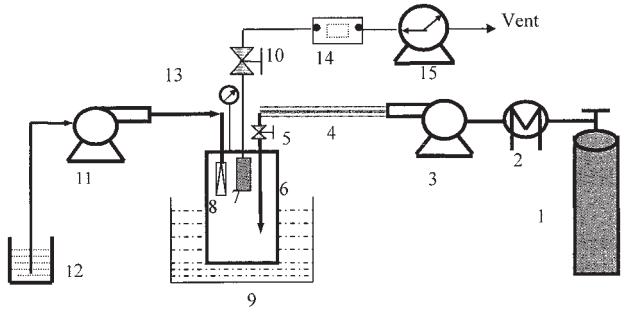

Figure 2. SAS coating process.

(1) CO_2 Cylinder; (2) refrigerator; (3) metering pump; (4) heating tape; (5) on-off valve; (6) precipitation chamber; (7) filter; (8) nozzle; (9) water bath; (10) metering valve; (11) HPLC pump; (12) suspension; (13) pressure gauge; (14) mass flow meter; (15) wet gas meter.

1000 mL. Its temperature was kept at the desired value using a water bath. The stainless steel capillary nozzle used to atomize the suspension, the CO_2 inlet, and the CO_2 outlet were all located on the lid of the precipitation chamber. The system pressure was controlled by a downstream metering valve (Swagelok, SS-31RS4, R.S. Crum & Co., Mountainside, NJ) and was monitored by a pressure gauge. Liquid CO_2 was supplied from a CO_2 cylinder by a metering pump (Model EL-1A, American Lewa®, Holliston, MA). A refrigerator (Neslab, RTE-111) was used to chill the liquefied CO_2 to around 0°C to avoid cavitation. The temperature of the liquefied CO_2 was then increased by using a heating tape (Berstead Thermolyne, BIH 171-100).

In running an experiment, the precipitation chamber was first charged with SC CO_2. When the desired operating conditions (temperature and pressure) were reached, a steady flow of CO_2 was established by adjusting the metering valve and the metering pump. The flow rate of CO_2 ranged from 1.0 to 5.0 standard liters per minute (SLPM). The coating material, PLGA, was then weighed and dissolved in the acetone–silica suspension to produce the desired polymer concentration and polymer to silica ratio. The prepared suspension was delivered into the precipitation chamber through a capillary nozzle (ID 254 μm) by using an HPLC pump (Beckman, 110B) for about 15 min. The flow rate varied from 0.4 to 1.3 mL/min.

After spraying, fresh CO_2 continued to flush the chamber to eliminate the organic solvent. In this washing step, the temperature and pressure were maintained under the same conditions as before. This washing step is necessary because any condensed organic solvent arising from phase separation between the organic solvent and SC CO_2 would redissolve the polymer on the surface of particles during depressurization. The washing step lasted about 3 h, depending on the process conditions. After the washing process, the precipitation chamber was slowly depressurized and the coated particles were harvested for characterization. The experimental operating conditions are listed in Table 2.

In the SAS coating experiments using a surfactant, a predetermined amount of surfactant was charged into the precipitation chamber before the experiment began. Once the predetermined processing conditions were achieved, the magnetic stirrer was turned on (600 rpm) to assist in the dissolution of the surfactant in SC CO_2. The experiment then followed the procedure described above. Table 3 lists the operating conditions for the SAS coating experiments using the surfactants.

Table 2. Experimental Operating Conditions without Surfactant

Run No.	T (°C)	P (MPa)	PLGA Conc. in Acetone (mg/mL)	PLGA Weight Fraction (%) of Coated Particles	Flow Rate (mL/min)	Observations
1	33.0	8.96	10.0	25.0	0.8	Fairly loose agglomerates
2	33.0	8.96	10.0	16.7	0.8	Very loose agglomerates
3	33.0	8.96	10.0	12.5	0.8	Very loose agglomerates
4	33.0	11.03	10.0	25.0	0.8	Heavily agglomerated (sintering)
5	38.0	8.96	10.0	16.7	0.8	Very loose agglomerates
6	42.5	8.96	10.0	16.7	0.8	Fairly loose agglomerates (some sintering)
7	33.0	8.96	4.0	16.7	0.8	No agglomerates observed
8	33.0	8.96	13.0	16.7	0.8	Loose agglomerates
9	33.0	8.96	10.0	16.7	1.8	Loose agglomerates
10	33.0	8.96	10.0	16.7	2.8	Loose agglomerates

Characterization

The silica particles were photographed using a field emission scanning electron microscope (FE-SEM; Leo, JSM-6700F) to observe any morphological changes before and after the coating treatment. The samples were either spread onto a carbon tape or onto an aluminum stub support device after dispersing in alcohol and evaporating. Particle size (PS) and particle size distribution (PSD) were analyzed using an LS Particle Size Analyzer (Beckman Coulter). Before particle size analysis, the coated and uncoated particles were dispersed in ethyl alcohol, in which the PLGA was not dissolved, and the resulting suspension was sonicated for 3 min. The sonicated suspension was then added to the Beckman Coulter sample cell one drop at a time.

To determine the amount of polymer that was coated onto the silica particles at different polymer weight fractions, thermogravimetric analyses were performed using a TGA apparatus (TA Instruments, New Castle, DE). In the TGA experiments, 3–5 mg of coated silica particles were used, the atmosphere was air, and the flow rate was 20 mL/min. The temperature was increased from room temperature to 500°C at a heating rate of 20°C/min, and then maintained at 500°C for 15 min so that the polymer on the surface of the particles would be completely burned off. The measured weight loss was assumed to consist entirely of polymer because the silica particles are inert at this temperature.

Table 3. Experimental Operating Conditions with Surfactant

T (°C)	P (MPa)	Surfactant	Surfactant Conc. (wt %) in SC CO_2	Observation
32.0	9.65	PFS	0.018	Dense film coating on the surface of vessel and stirrer
32.0	9.65	PFA	0.018	Dense film coating on the surface of vessel and stirrer
32.0	9.65	PFPE	0.018	Dense film coating on the surface of vessel and stirrer

Note: Polymer conc., 1.0% in acetone; polymer weight fraction of coated particles, 25.0%; flow rate, 0.8 mL/min.

Results and Discussion

SAS process fundamentals

The solubilities of the solute and solvent in SC CO_2 constitute important considerations in the SAS process. A successful SAS process requires good miscibility of the solvent and the SC CO_2, with the solute having negligible solubility in the SC CO_2. There is also a volumetric expansion when CO_2 is dissolved in the solvent, which is important for the precipitation of solute. The volumetric expansion $\Delta V\%$ is defined as

$$\Delta V\% = \frac{V(P, T) - V_0}{V_0} \times 100\% \tag{1}$$

where $V(P, T)$ is the volume of solvent expanded by CO_2 and V_0 is the volume of pure solvent.

In our system, we used acetone as the solvent and PLGA as the solute, respectively. Unfortunately, there are no experimental data available for the expansion rate and the solubility of PLGA in expanded acetone. However, the Peng–Robinson equation of state (PREoS)[17] can be used to predict the expansion behavior of the binary system of CO_2–acetone. The PREoS can be written as

$$P = \frac{RT}{v - b} - \frac{a(T)}{v(v + b) + b(v - b)} \tag{2}$$

where a and b are parameters of the mixture in the binary system. Originally, the PREoS had only one interaction coefficient, k_{ij}. However, as suggested by Kordikowski et al.,[18] it is necessary to have a second interaction parameter l_{ij} to account for a polar compound in the binary system. In our system, k_{ij} is -0.007 and l_{ij} is -0.002, which are regressed from the experimental data reported by Katayama et al.[19] The mixing rules are given as

$$a = \sum_i \sum_j x_i x_j a_{ij} \tag{3}$$

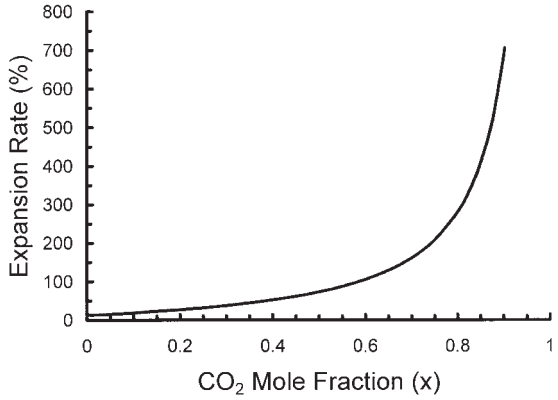

Figure 3. Volume expansion rate of acetone as a function of CO_2 mole fraction at 33.0°C.

$$b = \sum_i x_i x_j b_{ij} \tag{4}$$

$$a_{ij} = (1 - k_{ij}) \sqrt{a_i a_j} \tag{5}$$

$$b_{ij} = \frac{(b_i + b_j)}{2} (1 - l_{ij}) \tag{6}$$

where the pure component values can be determined as

$$b_{ii} = 0.07780 \frac{RT_{ci}}{P_{ci}} \tag{7}$$

$$a = 0.45724 \frac{R^2 T_{ci}^2}{P_{ci}} [1 + (0.37464 + 1.54226\omega_i - 0.26992\omega_i^2) \times (1 - \sqrt{T/T_{ci}})]^2 \tag{8}$$

and P_{ci}, T_{ci}, and ω_i are the critical pressure, critical temperature, and accentric factor of component i, respectively.

The calculated volume expansion rate as a function of the CO_2 mole fraction is shown in Figure 3. The volume of acetone increases slowly with CO_2 mole fraction, from 0 to 0.8. However, the volume expands significantly at higher CO_2 mole fraction. When the mole fraction is >0.85, the acetone is fully expanded. The expansion behavior of acetone results in a decrease in the partial molar volume of the solvent so that the solvent strength is reduced. To predict the solubility of PLGA in expanded acetone by CO_2, the partial molar volumes of each component $\bar{\nu}_i$ in the liquid phase needs to be calculated. These are obtained by differentiating the PREoS,[20] as follows:

$$\bar{\nu}_i = \frac{RT}{P} \left[Z + (1 - x_i) \left(\frac{\delta Z}{\delta x_i} \right)_{T,P} \right] \quad i = 1, 2 \tag{9}$$

where Z is the compressibility factor. The solubility of a solute in the liquid phase of the expanded solvent $S_3(T, P)$, is expressed as[21]

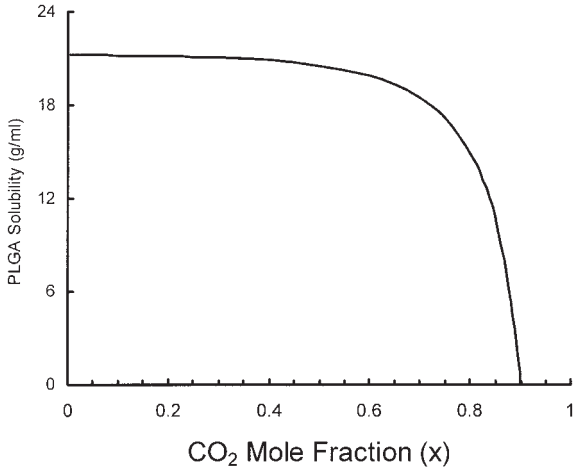

Figure 4. Solubility of PLGA in expanded acetone as a function of CO_2 mole fraction at 33.0°C.

$$S_3(T, P) = \frac{\bar{\nu}_2(T, P, x)}{\bar{\nu}_2(T, 1, 0)} S_3(T, 1) \tag{10}$$

where $S_3(T, 1)$ is the solubility at 1 atm, $\bar{\nu}_2(T, P, x)$ is the partial molar volume of solvent at T, P, and x, and $\bar{\nu}_2(T, 1, 0)$ is the partial molar volume of solvent at 1 atm and at the same temperature with no CO_2 dissolved.

The predicted solubility of PLGA in acetone expanded by CO_2 is shown in Figure 4. As seen in the figure, the solubility of PLGA in the liquid phase decreases as the CO_2 mole fraction is increased. When the CO_2 mole fraction is >0.7, the solubility decreases considerably. Above 0.85, the solubility of PLGA in acetone is negligible. The CO_2 molecules tend to surround the solvent molecules and reduce the partial molar volume of the solvent,[21] causing the decreased solvent strength.

A phase diagram is helpful to explain the SAS polymer coating process, although the overall process is very complicated because of the effects of hydrodynamics, kinetics, thermodynamics, and mass transfer, all of which need to be considered. Figure 5 shows a ternary phase diagram for the solvent–antisolvent–polymer. The three regions (S_1), (S_2) and (S_3) in the diagram, represent a single-phase region of polymer

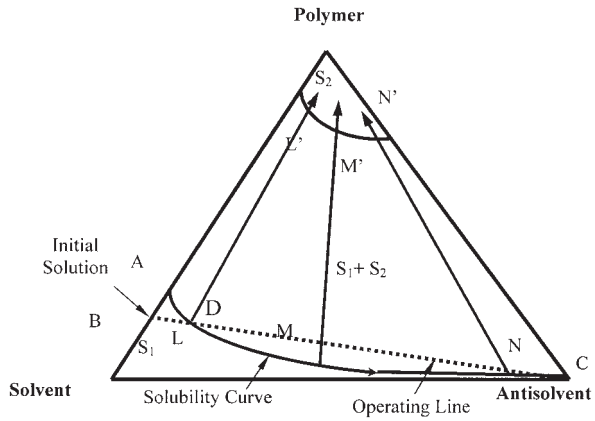

Figure 5. Schematic ternary phase diagram for solvent–polymer–antisolvent at constant *P* and *T*.

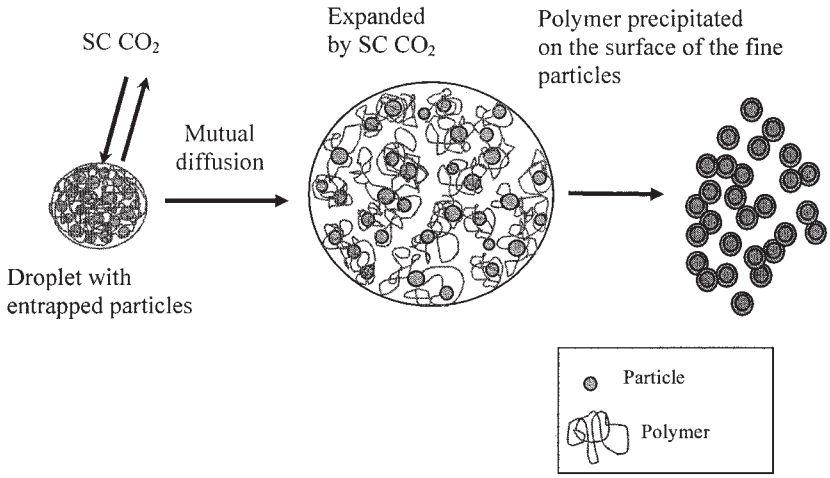

Figure 6. Cartoon of SAS process for fine particle encapsulation.

dissolved in acetone with some CO_2 absorbed, a single-phase region of mostly polymer with some acetone and CO_2 absorbed, and a two-phase region made up of the polymer-rich phase and the polymer-lean phase, respectively. The bold line is the solubility curve, representing the solubility of PLGA in the mixture of acetone and CO_2. The dotted line depicts the addition of polymer solution into SC CO_2.

When the acetone–polymer solution (suspended with silica particles) is pumped through a nozzle to form small droplets and contacts SC CO_2, a mutual diffusion between the SC CO_2 and the polymer solution occurs instantaneously. The SC CO_2 is dissolved in acetone, leading to swelling of the droplets.[22] With the continuing diffusion of SC CO_2 into polymer solution and acetone into SC CO_2, the polymer solution very quickly reaches saturation in the mixture of acetone and CO_2, as shown in Figure 5 (D, saturation point). Subsequently, the polymer solution forms two phases, a viscous polymer-rich phase with particles entrapped and a dilute polymer-lean phase (from D to C). Because the solubility of most polymers is very limited, it is reasonable to assume that the polymer-lean phase composition consists mostly of acetone and SC CO_2. As the mutual diffusion continues, the polymer-rich phase becomes more concentrated and more viscous. Further removal of solvent from the polymer-rich phase induces a phase transition to the glassy region (S_2) (lines from L to L′, M to M′, and N to N′). Eventually, the polymer vitrifies, forming a polymer film on the surface of particles. A cartoon illustrating the SAS process for fine particle encapsulation (as described above) is shown in Figure 6.

Coating of fine silica particles

High-resolution SEM microphotographs were taken to illustrate morphological changes before and after polymer coating. As seen in Figure 7, the synthesized silica particles are spherical and smooth on the surface. The PS and PSD of uncoated silica particles were determined using the LS Particle Size Analyzer. From Figure 8, the average PS of uncoated silica

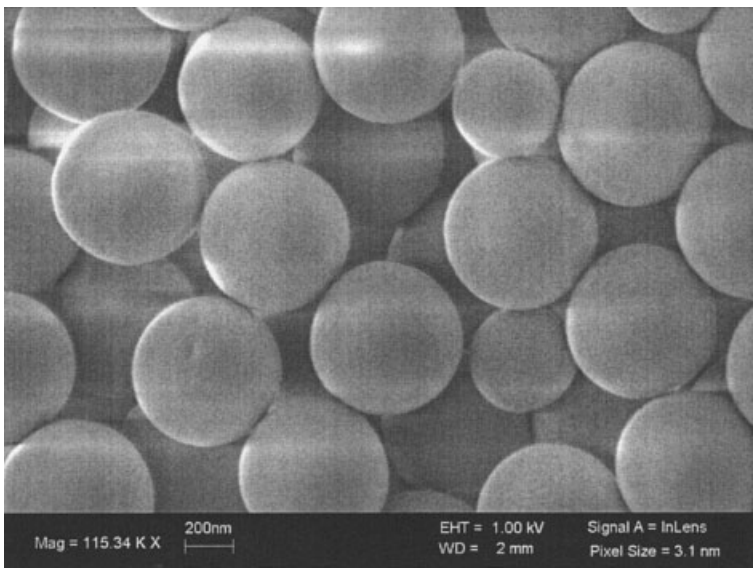

Figure 7. Spherical uncoated silica particles.

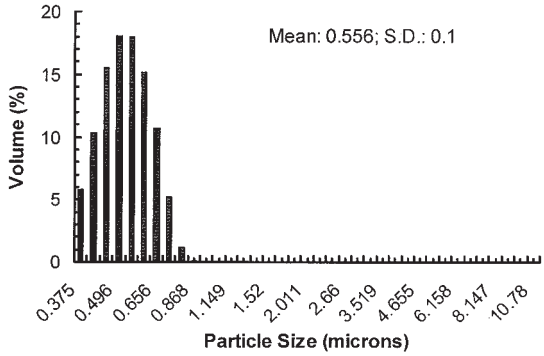

Figure 8. Particle size and particle size distribution of uncoated silica particles.

particles is 0.556 micron with a standard deviation of 0.1 micron.

Figure 9 shows the silica particles coated with polymer at a polymer fraction of 25.0% of the total coated particle mass. Compared with Figure 7, the coated silica particles (Figure 9a) exhibit a different morphology and surface feature. The coated particles are heavily agglomerated because of the polymer coating, which acts as a binder. During the precipitation of the polymer, the entanglement of polymer chains between neighboring particles binds them together, forming agglomerates as shown in Figure 9a. However, after sonication in alcohol for 3 min, the solid polymer bridges between the coated particles appeared to be broken, as shown in the outlined area in Figure 9b. In SEM, a high-intensity electron beam is used to scan the surface of particles. Because some of the kinetic energy of the electron beam is absorbed by the particles, the local temperature of the area that is scanned increases. Therefore, after the coated silica particles are exposed to the high-intensity electron beam for 15 min, the coating polymer becomes soft and spreads over the surface of particles (Figure 9c) because of the low glass-transition temperature of the polymer (40–55°C).

The quality of the coating and the degree of agglomeration were found to be affected by several operating parameters including the polymer weight fraction, polymer concentration in acetone, temperature, pressure, flow rate, and the addition of surfactants. These will be described in detail below.

Effect of polymer weight fraction

The amount of polymer applied in the coating of particles is important in controlling the coating thickness and agglomeration of the coated particles in the SAS process. The SAS coating process was operated at 33°C and 8.96 MPa, respectively, and the polymer weight fraction was varied from 12.5 to 25.0% (Runs 1, 2, and 3). SEM microphotographs of the coated particles at different polymer weight fractions (defined as the weight of polymer divided by the total weight of polymer and silica particles on a dry basis $\times$ 100) are shown in Figure 10. At a high polymer weight fraction of 25.0%, the coated particles were severely agglomerated (Figure 10a). When the polymer weight fraction was lowered to 16.7%, the agglomeration became much less pronounced (Figure 10b). When the polymer weight fraction was lowered even further to 12.5%, the agglomeration between the coated particles also appeared to decrease (Figure 10c).

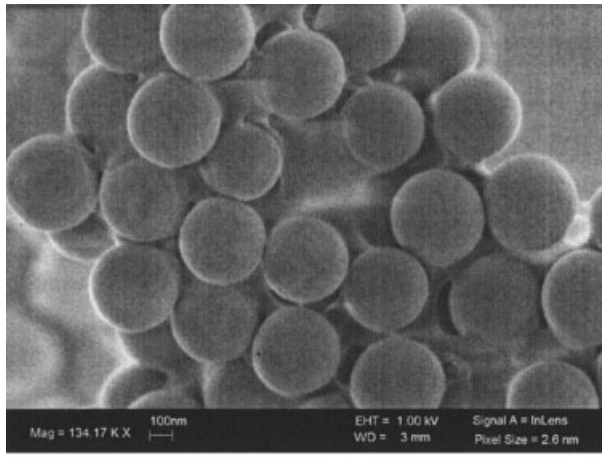

a

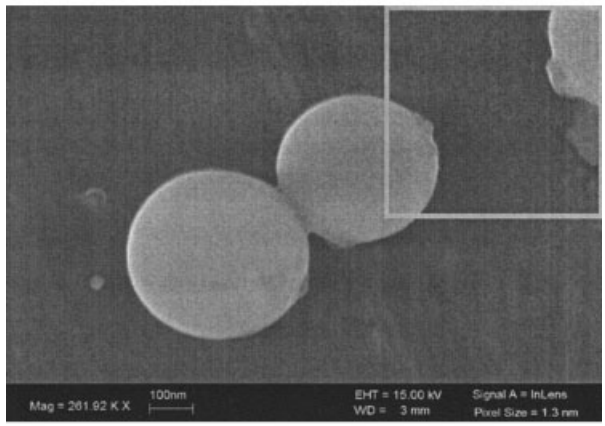

b

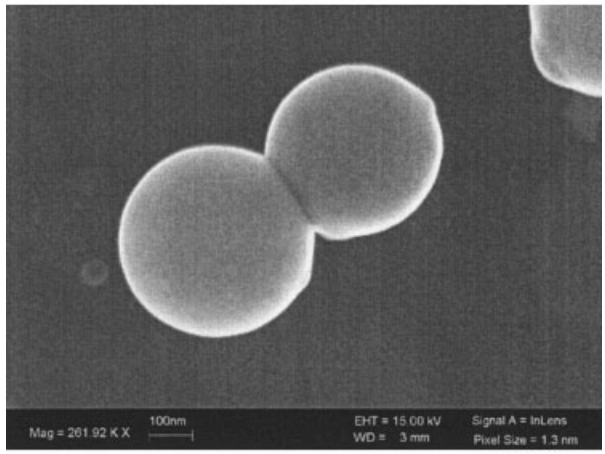

c

Figure 9. Coated silica particles at a polymer fraction of 25.0%.

(a) Coated silica particles before sonication; (b) coated silica particles after sonication for 3 min; (c) coated particles after being bombarded for 15 min with the electron beam.

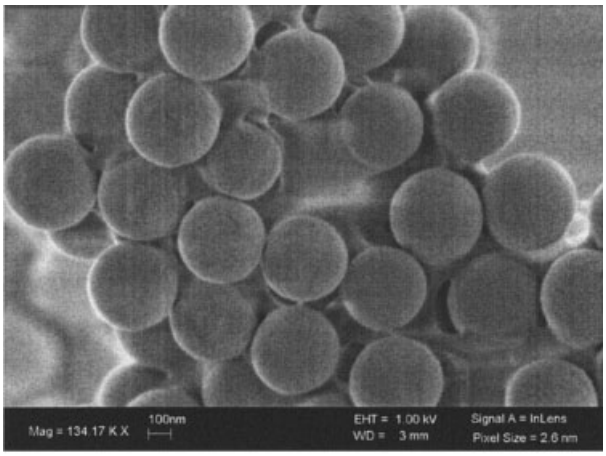

a

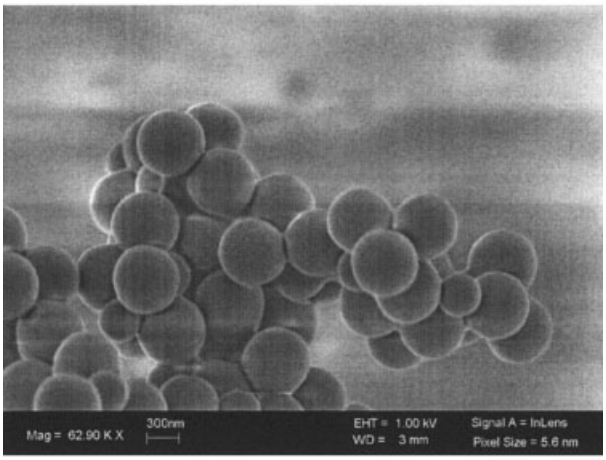

b

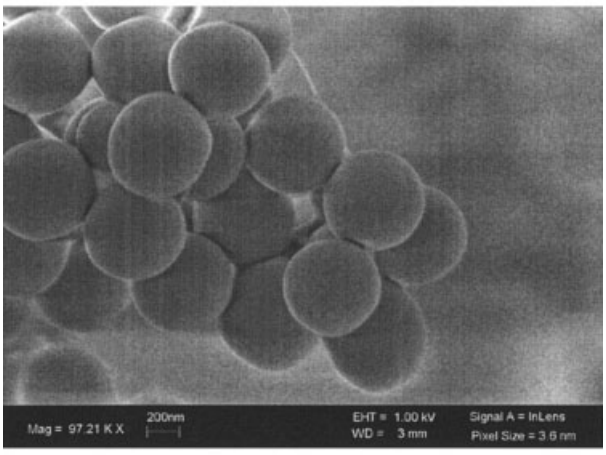

c

Figure 10. SEM microphotographs of coated particles at different polymer weight fractions.

(a) 25.0% (Run 1); (b) 16.7% (Run 2); (c) 12.5% (Run 3).

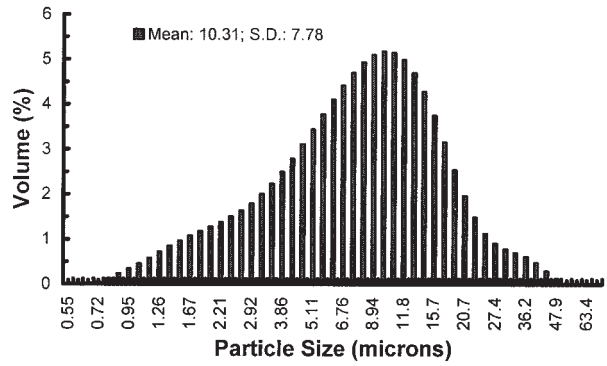

a

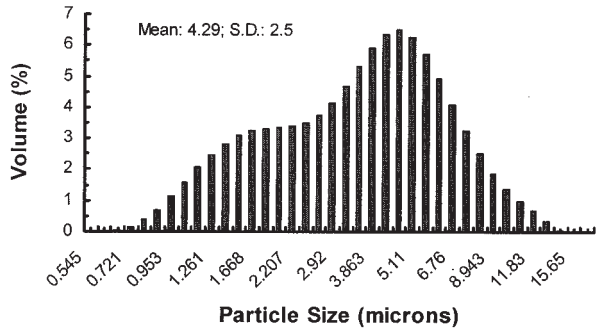

b

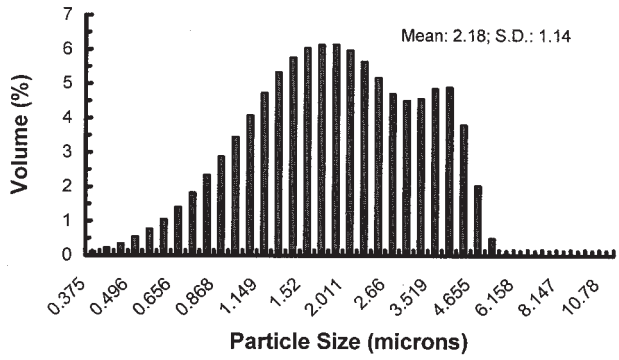

c

Figure 11. Average size and distribution of coated particles at different polymer weight fractions.

(a) 25.0% (Run 1); (b) 16.7% (Run 2); (c) 12.5% (Run 3).

The coated particles were analyzed in terms of particle size and particle size distribution to determine the degree of agglomeration. In measuring the particle size and particle size distribution, the coated particles were dispersed in ethyl alcohol. The resulting suspension was sonicated for 3 min. Figure 11 shows the results of the particle size and particle size distribution at different polymer weight fractions. The average size of agglomerates of coated particles at the fraction of 25.0% is 10.31 microns with a standard deviation of 7.78 microns, as shown in Figure 11a. It is obvious that agglomeration among the coated particles occurred because the average size of the

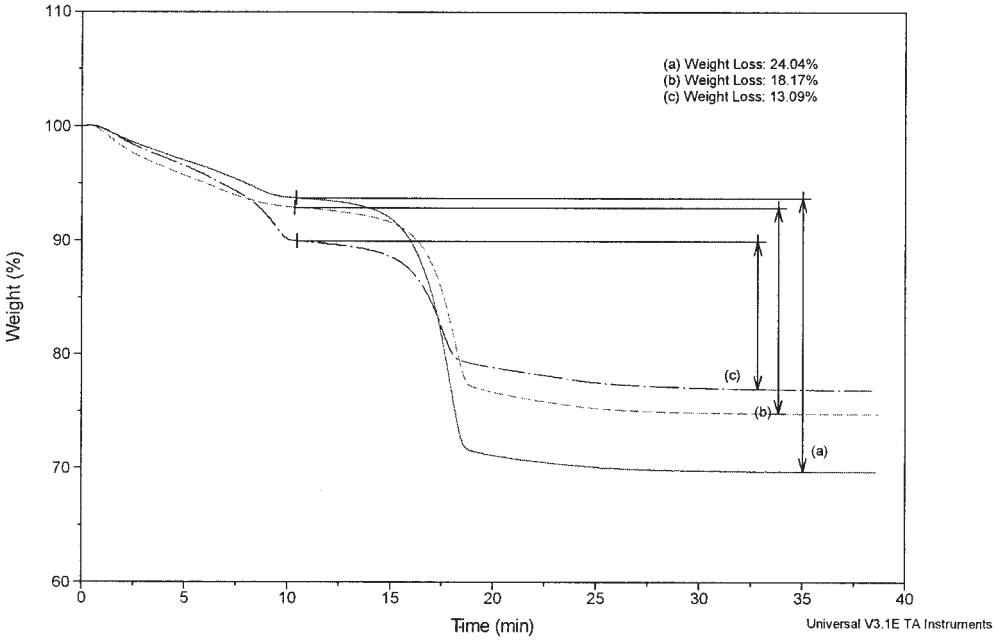

Figure 12. Weight loss profiles of coated silica particles at different weight fractions.

uncoated particles is 0.556 microns with a narrow size distribution of 0.1 micron. This is consistent with the observation in Figure 10a. The average size of agglomerates of coated particles decreased considerably, to 4.29 microns with a distribution of 2.5 microns, when the particles were coated at the polymer weight fraction of 16.7% (Figure 11b). When the weight fraction was reduced to 12.5%, the average size of agglomerates of coated particles decreased to 2.18 microns with a distribution of 1.14 microns. There is a good agreement between the SEM microphotographs in Figure 10 and the results of particle size and particle size distribution analysis using the Beckman Coulter LS Particle Size Analyzer in Figure 11.

The amount of polymer coated on the silica particles at different weight fractions was analyzed using TGA. TGA curves of pure polymer and silica particles coated at different weight fractions are shown in Figure 12. The pure polymer (PLGA) started to decompose at about 200°C. When the temperature was increased to 500°C and held for 15 min, the PLGA was totally burned off and the TGA curve leveled off. The TGA curve of coated particles at a weight fraction of 25% showed a 24.3% weight loss. This is very close to the theoretical polymer loading. Similarly, the TGA curves of coated samples at polymer weight fractions of 16.7 and 12.5% show weight losses of 18.4 and 13.4%, respectively, and are also fairly consistent with the theoretical polymer loadings.

Effect of polymer concentration

Polymer concentration (defined as the weight of polymer divided by the volume of organic solvent used) was found to be very important in controlling the agglomeration of coated particles in the SAS process. The polymer concentration was varied from 4.0 to 13.0 mg/mL while keeping all other operating parameters constant (Runs 2, 7, and 8). SEM microphotographs of coated particles at different concentrations are shown in Figure 12. At high polymer concentration of 13 mg/mL, the coated particles were heavily agglomerated. In addition, the polymer coating on the surface of particles was found to be unevenly distributed (Figure 13a). When the polymer concentration decreased to 10.0 mg/mL, the polymer coating on the surface of particles appeared smoother. Nevertheless, agglomeration of coated particles can be seen in Figure 13b. A further decrease in the polymer concentration to 4.0 mg/mL showed smooth particle coating with minimal agglomeration, as seen in Figure 13c.

The results of the particle size analysis of the coated particles at different polymer concentrations are shown in Figure 14. Although the polymer weight fraction was maintained at 16.7%, a higher polymer concentration results in larger agglomerates. When particles were coated at a polymer concentration of 13.0 mg/mL, the average size of agglomerates is 7.45 microns with a distribution of 4.03 microns (Figure 14a). However, the average size of agglomerates decreased to 4.29 microns when the polymer concentration was reduced to 10.0 mg/mL (Figure 14b). When the polymer concentration was lowered further to 4.0 mg/mL, the average size of agglomerates decreased significantly to 0.613 microns with a distribution of 0.135 microns (Figure 14c). Thus it appears that no agglomeration occurred, and the increase in average particle size is simply a result of the polymer coating on the surface of the particles. The coating thickness is estimated to be 28.5 nm based on the measurements of uncoated particles and coated particles at a polymer concentration of 4.0 mg/mL.

The thickness of the coating layer on the surface of the particles can also be estimated from the polymer weight fraction. If it is assumed that no agglomeration occurs, that the PLGA coats the only silica particles and the coating is uniform on the surface of a particle with a thickness t, then

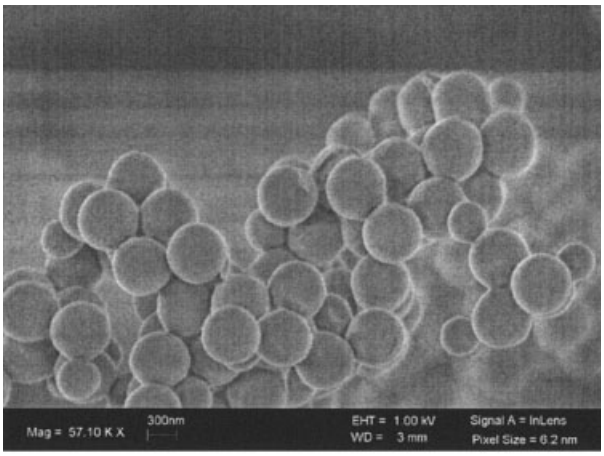

a

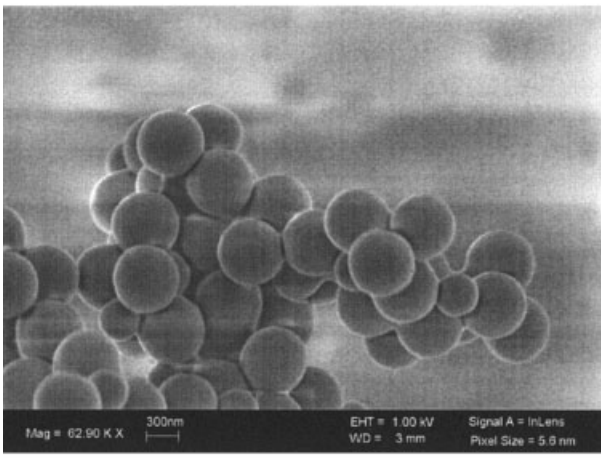

b

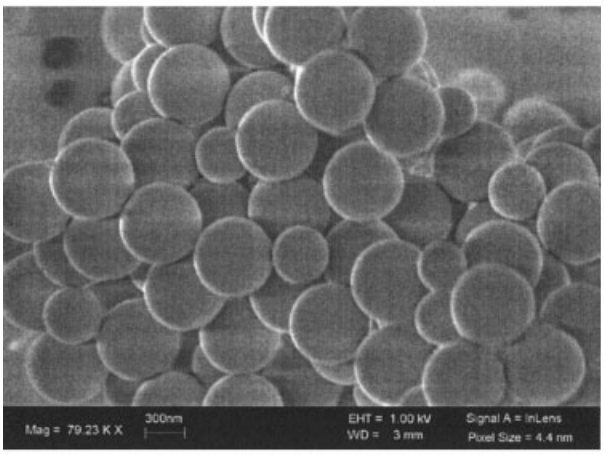

c

Figure 13. SEM microphotographs of coated particles at different polymer concentrations.

(a) 13.0 mg/mL (Run 8); (b) 10.0 mg/mL (Run 2); (c) 4.0 mg/mL (Run 7).

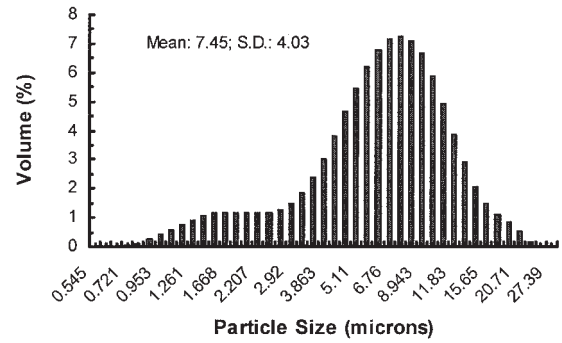

a

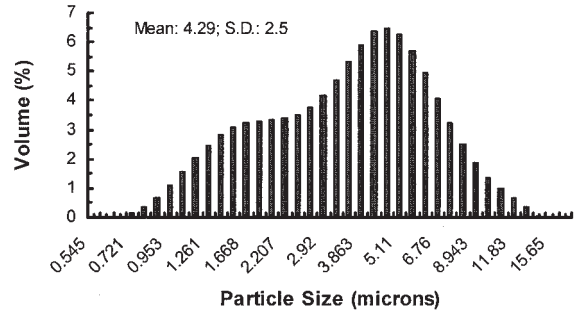

b

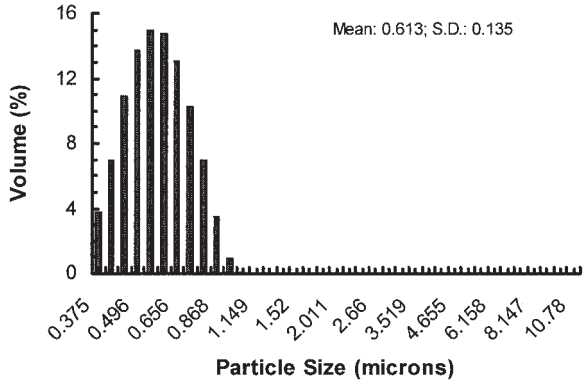

c

Figure 14. Average size and size distribution of coated particles at different polymer concentrations.

(a) 13.0 mg/mL (Run 8); (b) 10.0 mg/mL (Run 2); (c) 4.0 mg/mL (Run 7).

$$t = R(1 + \rho_H m_C/\rho_C m_H)^{1/3} - R \qquad (11)$$

where R is the radius of the uncoated particle; ρ_H and ρ_C are the densities of the host particles and PLGA, respectively; and m_H and m_C are the weights of the host particles and polymer, respectively. Knowing the polymer weight fraction and using Eq. 11, t is estimated to be 29 nm, which is very close to the value obtained from the size measurements of the uncoated particles and coated particles. This calculation strongly supports the conclusion drawn above that no agglomeration among coated particles occurs when using a polymer concentration of 4.0 mg/mL.

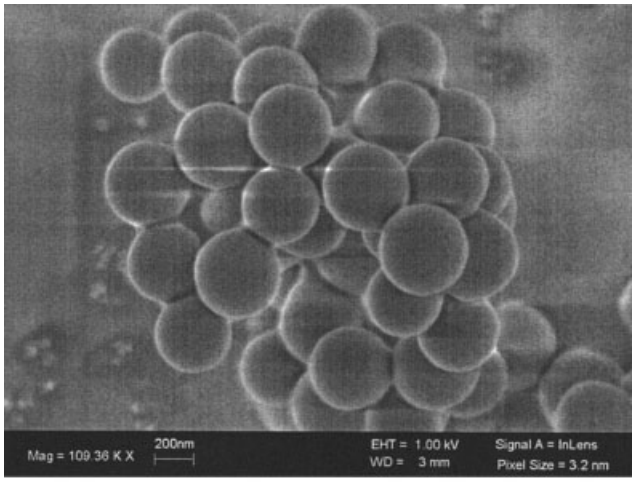

a

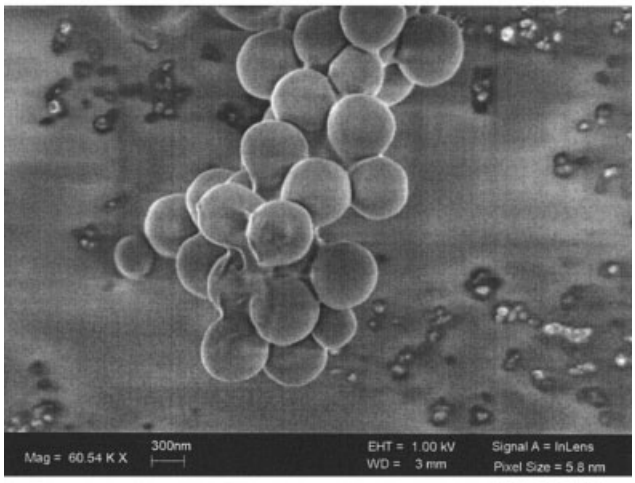

b

Figure 15. SEM microphotographs of coated particles at different temperatures.

(a) 38°C (Run 5); (b) 42.5°C (Run 6).

Effect of temperature

In previous studies using the SAS process for particle formation,[22-24] the operating temperature was found to affect both the particle size and morphology of the final product. Because the SAS process for particle formation, and that for particle coating used here, are very similar, except that for coating the host particles are suspended in the polymer solution before being delivered into SC CO_2, it is likely that temperature will have an effect on the coating and agglomeration of the coated particles. To determine the temperature effect the experiments were carried out at different temperatures from 33 to 42.5°C while the other operating parameters were kept constant (Runs 2, 5, and 6). Figure 13 and Figure 15 show SEM microphotographs of the coated particles at different temperatures.

Below the glass-transition temperature of PLGA (T_g = 40–55°C), the coated particles at 33 and 38°C appear to be very similar. The average size of the agglomerates at 33°C is 4.29 microns with a distribution of 2.5 microns (Figure 14b), and at 38°C, 4.61 microns with a distribution of 3.25 microns (Figure 16a). There is only a very slight increase in agglomerate size with temperature. However, when the operating temperature is increased to 42.5°C, above the glass-transition temperature of PLGA, the coated particles were heavily agglomerated, as seen in Figure 16b, as a result of sintering. In addition, the polymer coating is very unevenly distributed on the surfaces of the host particles. A particle size measurement of the coated particles at 42.5°C shows that the average size of the agglomerates increases significantly from about 4.5 to 12.9 microns (Figure 16b). Therefore we can conclude that T_g of the polymer plays a key role in the agglomeration of the coated particles.

Effect of pressure

The pressure of the system is one of the most important variables in the SAS process because it affects the density of SC CO_2. Thus, the rate of mutual diffusion between SC CO_2 and the polymer solution will be influenced. Furthermore, Mawson et al.[25] and Condo et al.[26] found that the glass-transition temperature of polymers could be severely depressed by compressed CO_2. For example, Condo et al.,[26] reported that T_g of PMMA could be depressed 100°C below its normal value of 105°C under a high pressure of CO_2. To examine the effect

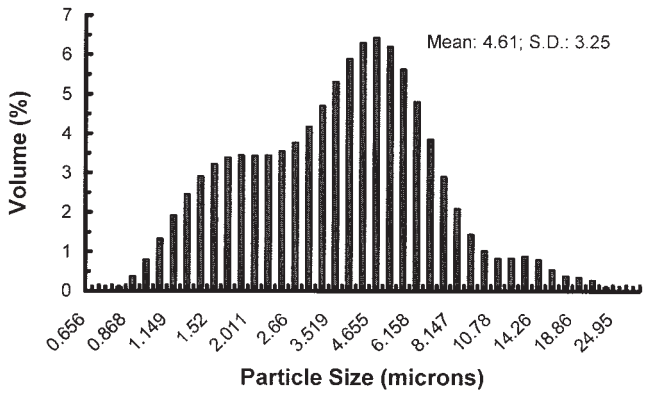

a

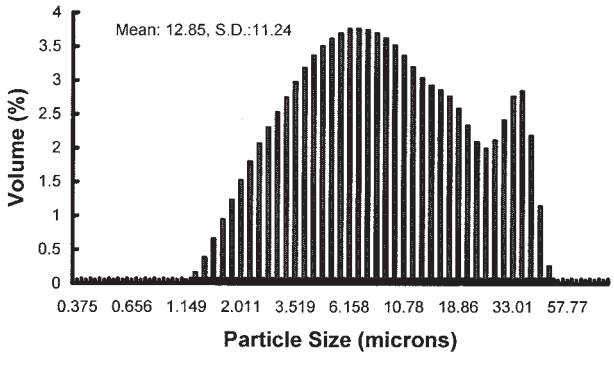

b

Figure 16. Average size and size distribution of coated particles at different temperatures.

(a) 38°C (Run 5); (b) 42.5°C (Run 6).

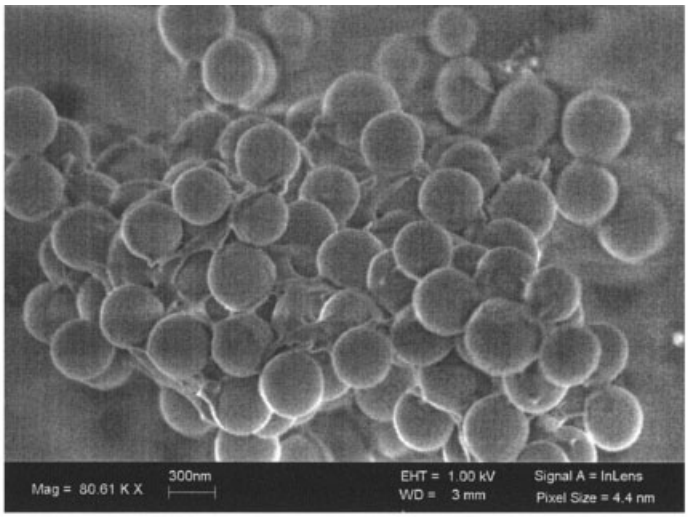

a

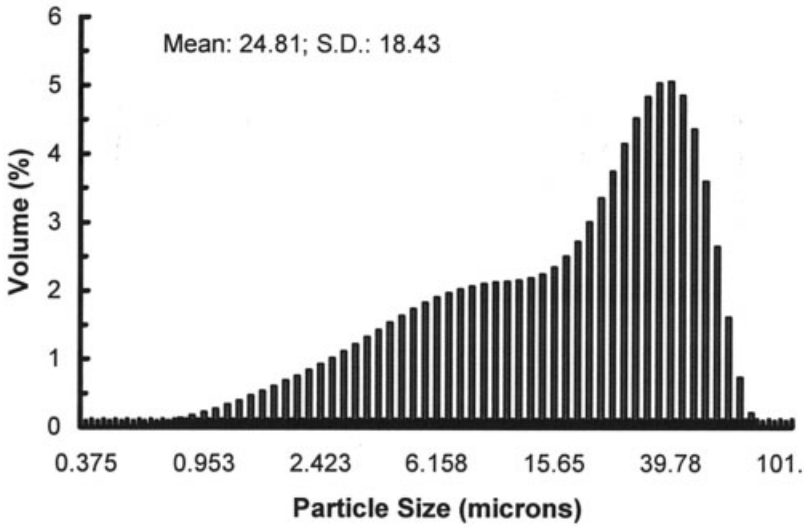

b

Figure 17. SEM microphotographs (a) and average size of agglomerates (b) of coated particles at a pressure of 11.03 MPa (Run 4).

of pressure, experiments were carried out at two different operating pressures of 8.96 and 11.03 MPa while the temperature was kept constant at 33°C (Runs 1 and 4). Figure 17a shows a SEM microphotograph of coated particles under a pressure of 11.03 MPa. The coated particles were heavily agglomerated compared with the coated particles seen in Figure 10a at 8.96 MPa. In addition, it was found that the polymer coating was unevenly distributed.

The average size of the agglomerates increased to 24.8 microns with a distribution of 18.4 microns, as shown in Figure 17b. This may be attributable to a depression in T_g of the polymer in pressurized CO_2. The agglomeration of coated particles appears to be enhanced by plasticization of the coating polymer under high pressure. The degree of plasticization of polymer is proportional to the amount of CO_2 absorbed into the polymer matrix, that is, proportional to the operating pressure. This explains why the agglomeration of coated particles at 11.03 MPa is much worse than that at 8.96 MPa. Also, T_g depression appears to favor a redistribution of polymer coating on the surface of particles, as seen in Figure 17a.

Effect of flow rate

In SAS particle formation, the flow rate of the solution has been reported to have an effect on the particle size and morphology of final products.[22,27,28] To study the effect of flow rate in our SAS coating process, experiments were performed at different flow rates, varying from 0.8 to 2.8 mL/min (Runs 2,

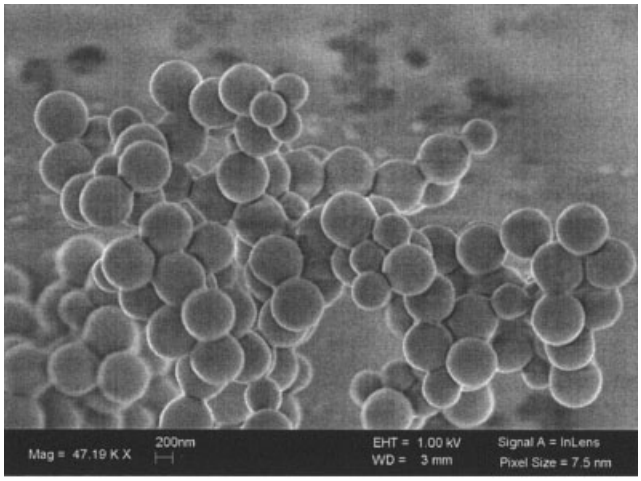

a

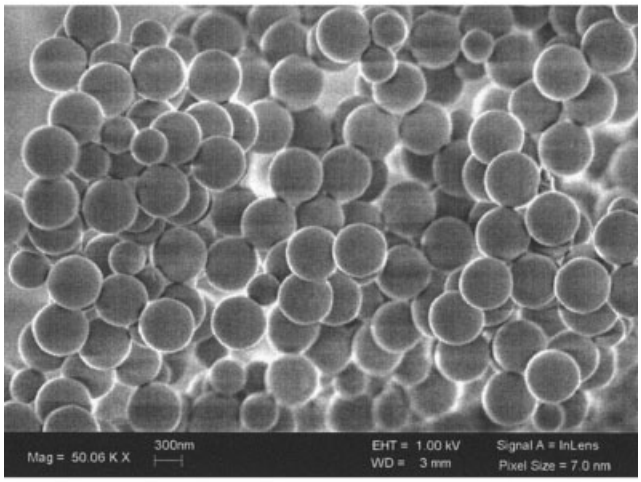

b

Figure 18. SEM microphotographs of coated particles at different flow rates.

(a) 1.8 mL/min (Run 9); (b) 2.8 mL/min (Run 10).

9, and 10). The SEM microphotographs of the coated particles are shown in Figure 10b and Figure 18. The surface of the coated particles at the three different flow rates is fairly smooth and there does not appear to be any difference in the degree of agglomeration arising from changes in flow rate.

The particle size measurements are shown in Figure 11b and Figure 19. No clearly defined trend can be observed from these figures, except that the average size of the agglomerates at a flow rate of 2.8 mL/min is slightly increased. Thus it appears that flow rate plays a less critical role in the coating of particles in the SAS process compared to other operating parameters, such as polymer concentration, polymer weight fraction, temperature, and pressure, which were discussed above. However, the concentration of the organic solvent in the suspension droplets extracted by SC CO_2 should be sufficiently low so that the polymer coating on the surface of the silica particles solidifies before contacting other coated particles or the surface of the vessel. Otherwise, agglomeration would take place when the viscous liquid polymer coatings on the surface of particles contact each other. Therefore, the flow rate should be lower than a certain limiting value to prevent agglomeration.

Effect of surfactants

To evaluate the effect of surfactants in the SAS coating process, we used various surfactants that are fully soluble in SC CO_2 at the concentration, temperature, and pressure of interest. The fluoroalkyl side chains of polyfluoroalkyl acrylate (PFA)[29] and poly(fluoroalkyl acrylate-*co*-styrene) (PFS)[30] polymers and the polyfluoroether tail of the poly(perfluorofluorether) carboxylic acid (Krytox 157 FS)[31] are known to be CO_2-philic and were expected to interact favorably with the SC CO_2. It was conjectured that the CO_2-phobic backbone of PFA, the backbone and pendant aromatic groups of the PFS, and the carboxylic acid of the Krytox 157 FS could coat the PLGA surface.

Before starting an experiment, a known amount of surfactant was charged to a high-pressure chamber. To compare the effect of surfactants to reduce agglomeration of the coated particles, the operating conditions were chosen to be the same as in the coating experiments without using any surfactants. When the desired experimental conditions were reached, the magnetic

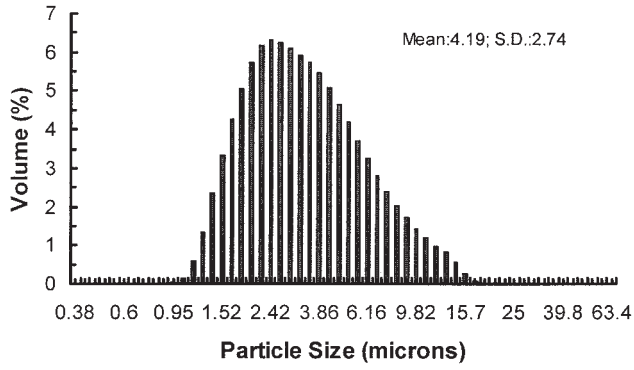

a

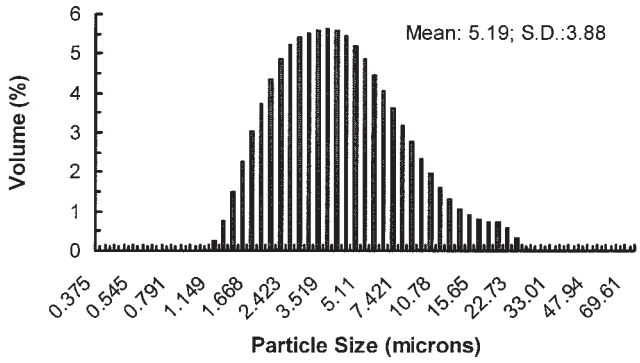

b

Figure 19. Average size and size distribution of coated particles at different flow rates.

(a) 1.8 mL/min (Run 9); (b) 2.8 mL/min (Run 10).

stirrer was turned on (300–600 rpm) to facilitate the dissolution of the surfactant. After about 30 min of agitation, the surfactant was assumed to be completely dissolved in SC CO_2. The suspension of particles in polymer solution was then supplied by the HPLC pump through the nozzle into SC CO_2 with the surfactant presumed to be dissolved. The subsequent steps of flushing with fresh CO_2 and depressurization are the same as those in the SAS coating experiments without surfactants.

In examining the literature of dispersion polymerization in SC CO_2, it was found that the effective concentration of surfactants used was usually in the range of 0.1 to 2.0 wt % in CO_2 at 65°C and >34 MPa.[32-35] In a recent study of dye impregnation microencapsulation for latices using CO_2, a surfactant, Pluronic F108, was used to effectively disperse the dyes by emulsifying CO_2–water and CO_2–ethanol systems at concentrations from 0.1 to 1.5% at 25°C and 31 MPa.[36] Because the pressure used in the SAS coating experiments is 8.96 MPa, much lower than the pressures used in the dispersion polymerization and impregnation work, a concentration of 0.1% of PFA surfactant in SC CO_2 was initially tried. However, the surfactant, which is known to dissolve very slowly in SC CO_2 even when agitated,[30] was found not to have been completely dissolved because surfactant particles were observed inside the vessel after disassembly of the high-pressure chamber.

In a PCA microparticle formation study done by Mawson et al.[37] the effective surfactant concentration to stabilize polymer microparticles was found to be in the range of 0.01 to 0.05%, depending on which surfactants were introduced into CO_2 at operating conditions of 23°C and 14.9 MPa. Therefore, the amount of surfactant was reduced to 0.0185% and the pressure raised from 8.96 to 9.65 MPa. However, once again the surfactants were found not to completely dissolve in SC CO_2, even at the lower concentration.

When the coating experiment was completed (using PFA), no free-flowing particles or agglomerates were found inside the chamber. Instead, a film coating occurred on the surface of the chamber, and on the surface of the stirrer as well. The film coating was scraped from the surface and was observed underneath the SEM. Figure 20a shows the coated particles scraped from the surface of the vessel in the SAS coating experiment with the addition of PFA surfactant. It can be seen that the coated particles are very heavily agglomerated. Furthermore, the coating is found to be very different compared with that in Figure 10a, even though the polymer weight fraction is the same. In a separate experiment to measure the solubility of PFA in SC CO_2, it was observed in a high-pressure view cell that some of the PFA was dissolved and some was liquefied by SC CO_2 at these operating conditions. Therefore, it is hypothesized that the coated particles might have been wet by the liquefied PFA. After depressurization, the PFA solidified and formed solid bridges among the coated particles, resulting in extensive agglomeration.

To further evaluate the effect of the surfactant, the SAS coating experiment using PFA at the same concentration (0.0185%) was operated at a higher pressure of 12.1 MPa and temperature of 32°C. It was confirmed in a high-pressure view cell that the PFA was fully dissolved in SC CO_2 at these conditions. However, the result (not shown) turned out to be even worse than the coating experiment at 9.65 MPa. At the higher pressure a molecular interaction between PLGA and

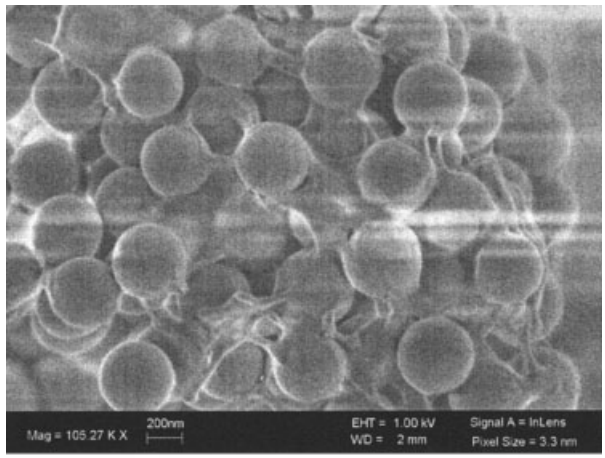

a

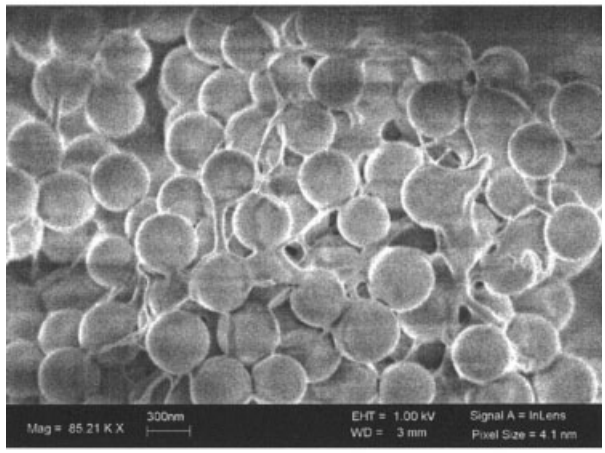

b

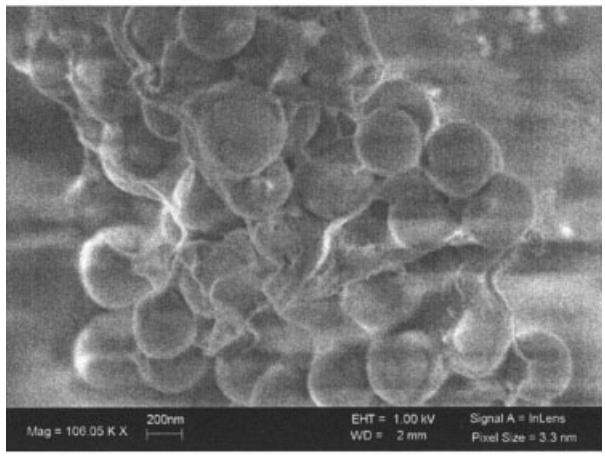

c

Figure 20. SEM microphotographs of coated particles using surfactants.

(a) PFA; (b. PFS, (c) Krytox. Polymer weight fraction 25.0%, polymer conc. 10 mg/mL, flow rate, 0.8 mL/min.

PFA might have occurred because they both have –COO– groups. A molecular attraction may cause the backbone of PFA to stick to PLGA, whereas the pendent CO_2-philic fluoroalkyl groups extend into the SC CO_2 phase. After depressurization, the CO_2-philic fluoroalkyl chains may intertwine and collapse, forming a network and binding the coated particles together. Alternately, the PFA would have liquefied upon initial depressurization, wetting the particles, and then solidified upon continued depressurization, causing the particles to agglomerate.

The coating experiment with PFA as a surfactant was also performed at a much lower concentration of 0.00185%, one-tenth the previous value. However, the result was the same.

Two other SC CO_2 soluble surfactants, PFS and Krytox, were also used following the same experimental procedure as with PFA at the concentration of 0.0185%. Again, particle coating on the surface of the vessel and stirrer was found in both experiments. SEM microphotographs of the coated products from these experiments are shown in Figures 20b and c, respectively. Clearly, the coated particles are very heavily agglomerated in both cases because of interactions between the surfactants and the PLGA.

Because none of the SC CO_2 soluble surfactants was effective, two other surfactants, poly(dimethyl-siloxane) (PDMS)[32] and block copolymer poly(propylene oxide)–poly(ethylene oxide)–poly(propylene oxide) (PPO–PEO–PPO, Pluronic 25R2),[36,37] which are soluble in acetone and in SC CO_2, were tried. These surfactants were dissolved in the coating polymer solution because they are soluble in acetone and were sprayed into SC CO_2 along with the silica particles and the coating solution. The results showed that the coatings, with or without either of these surfactants present, were similar; no effect on the minimization of agglomeration of coated particles was observed.

Concluding Remarks

Particle coating with polymer using the SAS process with SC CO_2 was systematically studied. Our results show that submicron silica particles were successfully coated or encapsulated by PLGA in the form of loose agglomerates. It was found that the polymer weight fraction and the polymer concentration play critical roles in the agglomeration of the coated particles. A high polymer weight fraction favors the agglomeration of the coated particles and the uneven distribution of the polymer coating. A low polymer concentration of 4.0 mg/mL appears to prevent agglomeration among the coated particles. The operating pressure and temperature were also found to influence agglomeration. A higher pressure facilitates the agglomeration of coated particles as a result of sintering because the glass-transition temperature of the polymer, T_g, is depressed. The operating temperature appeared to have little effect on the agglomeration of the coated particles when the temperature is below the glass-transition temperature; however, when the operating temperature is above T_g, the polymer coating on the surface of particle appears to be sintered, causing strong agglomeration. The flow rate of the polymer suspension was found to have little effect on the agglomeration.

Five surfactants—PFA, PFS, Krytox, PDMS, and Pluronic 25R2, all soluble in SC CO_2—were used in the hope that they would suppress agglomeration of the coated particles in the SAS process. However, the results showed that the PDMS and Pluronic 25R2 surfactants, which are also soluble in acetone, had no effect on minimizing agglomeration of the coated particles. The PFA, PFS, and Krytox surfactants, surprisingly, actually facilitated agglomeration.

Acknowledgments

The authors thank the National Science Foundation (NSF) for financial support through Grant CTS-9985618, and the New Jersey Commission of Science and Technology for financial support through Award 01-2042-007-24. Electron microscopy imaging was made possible in part through an MRI grant from the NSF (CTS-0116595). Thanks are also due to the staff of the Materials Characterization Laboratory at NJIT.

Literature Cited

1. Davies R, Schur GA, Meenan P, Nelson RD, Bergna HE, Brevett CA, Goldbaum RH. Engineered particle surface. *Adv. Mater.* 1998;10:1264-1270.
2. Wang D, Robinson DR, Kwon GS, Samuel J. Encapsulation of plasmid DNA in biodegradable poly(D,L-lactic-*co*-glycolic acid) microspheres as a novel approach for immunogene delivery. *J. Controlled Release.* 1999;57:9-18.
3. Soppimath KS, Kulkarni AR, Aminabhavi TM. Encapsulation of antihypertensive drugs in cellulose-based matrix microspheres: Characterization and release kinetics of microspheres and tableted microspheres. *J. Microencapsul.* 2001;18:397-409.
4. Tom JW, Debenedetti PG. Precipitation of poly(L-lactic acid) and composite poly(L-lactic acid)-pyrene particles by rapid expansion of supercritical solutions. *J. Supercrit. Fluids.* 1994;7:9-29.
5. Kim JH, Paxton TE, Tomasko DL. Microencapsulation of naproxen using rapid expansion of supercritical solutions. *Biotechnol. Prog.* 1996;12:650-661.
6. Mishima K, Matsuyama K, Tanabe D, Yamauchi S, Young TJ, Johnston KP. Microencapsulation of proteins by rapid expansion of supercritical solution with a nonsolvent. *AIChE J.* 2000;46:857-865.
7. Wang Y, Wei D, Dave R, Pfeffer R, Sauceau M, Letourneau J-J, Fages J. .Extraction and precipitation particle coating using supercritical CO_2. *Powder Technol.* 2002;127:32-44.
8. O'Neill ML, Cao Q, Fang M, Johnston KP, Wilkinson SP, Smith C, Kerschner JL, Jureller SH. Solubility of homopolymers and copolymers in carbon dioxide. *Ind. Eng. Chem. Res.* 1998;37:3067-3079.
9. Pessey V, Mateos D, Weill F, Cansell F, Etourneau J, Chevalier B. $SmCo_5$/Cu particles elaboration using a supercritical fluid process. *J. Alloys Compd.* 2001;323:412-416.
10. Pessey V, Garriga R, Weill F, Chevalier B, Etourneau J, Cansell F. Core-shell materials elaboration in supercritical mixture CO_2/ethanol. *Ind. Eng. Chem. Res.* 2000;39:4714-4719.
11. Chang CJ, Randolph AD. Precipitation of microsized organic particles from supercritical fluids. *AIChE J.* 1989;35:1876-1882.
12. Matson DW, Fulton JL, Peterson RC, Smith RD. Rapid expansion of supercritical fluid solutions: Solution formation of powders, thin films, and fibers. *Ind. Eng. Chem. Res.* 1987;26:2298-2306.
13. Tom JW, Debenedetti PG. Formation of bioerodible polymeric microspheres and microparticles by rapid expansion of supercritical solutions. *Biotechnol. Prog.* 1991;7:403-411.
14. Young TJ, Johnston KP, Mishima K, Tanaka H. Encapsulation of lysozyme in a biodegradable polymer by precipitation with a vapor-over-liquid antisolvent. *J. Pharm. Sci.* 1999;88:640.
15. Wang Y, Dave R, Pfeffer R. Nanoparticle encapsulation with heterogeneous nucleation in a supercritical antisolvent process. *J. Supercrit. Fluids.* 2004;28:85-99.
16. Stöber W, Fink A, Bohn E. Controlled growth of monodisperse silica spheres in the micron size range. *J. Colloid Interface Sci.* 1968;26:62-69.
17. Peng D-Y, Robinson DB. A new two-constant equation of state. *Ind. Eng. Chem. Fundam.* 1976;15:59-64.
18. Kordikowski A, Schenk AP, Van Nielen RM, Peters CJ. Volume expansions and vapor–liquid equilibria of binary mixtures of a variety of polar solvents and certain near-critical solvents. *J. Supercrit. Fluids.* 1995;8:205-216.
19. Katayama T, Ohgaki K, Maekawa G, Goto M, Nagano T. Isothermal vapor–liquid equilibria of acetone–carbon dioxide and methanol car-

bon dioxide systems at high pressures. *J. Chem. Eng. Jpn.* 1975;8:89-92.
20. Walas SM. *Phase Equlibria in Chemical Engineering*. Boston, MA: Butterworth; 1985:chap. 2.
21. Chang CJ, Randolph AD. Solvent expansion and solute solubility predictions in GAS-expanded liquids. *AIChE J.* 1990;36:939-942.
22. Randolph TW, Randolph AJ, Mebes M, Young S. Sub-micrometer-sized biodegradable particles of poly(L-lactic acid) via the gas antisolvent spray precipitation process. *Biotechnol. Prog.* 1993;9:429.
23. Reverchon E, Della Porta G, Di Trolio A, Pace S. Supercritical antisolvent preparation of nanoparticles of superconductor precursors. *Ind. Eng. Chem. Res.* 1998;37:952-958.
24. Yeo SD, Lim G-B, Debenedetti PG, Bernstein H. Formation of microparticle protein powders using supercritical fluid antisolvent. *Biotechnol. Bioeng.* 1993;41:341-346.
25. Mawson S, Johnston KP, Betts DE, McClain JB, DeSimone JM. Stabilized polymer microparticles by precipitation with a compressed fluid antisolvent: 1. Poly(fluoro acrylates). *Macromolecules*. 1997;30:71-77.
26. Condo PD, Paul DR, Johnston KP. Glass transition of polymers with compressed fluid diluents: Type II and III behavior. *Macromolecules.* 1994;27:365-371.
27. Chattopadhyay P, Gupta RB. Supercritical CO_2 based production of fullerence nanoparticles. *Ind. Eng. Chem. Res.* 2000;39:2281-2289.
28. Tu LS, Dehghani F, Foster NR. Micronisation and microencapsulation of pharmaceuticals using a carbon dioxide antisolvent. *Powder Technol.* 2002;126:134-149.
29. Blasig A, Shi C, Enick RM, Thies MC. Effect of concentration and degree of saturation on RESS of a CO_2-soluble fluoropolymer. *Ind. Eng. Chem. Res.* 2002;41:4976-4983.
30. Xu J, Wlaschin A, Enick RM. Thickening carbon dioxide with the fluoroacrylate—styrene copolymer. *SPE J.* 2003;8:85.
31. Hoefling TA, Beitle RR, Enick RM, Beckman EJ. Design and synthesis of highly CO_2-soluble surfactants and chelating agents. *Fluid Phase Equilib.* 1993;83:203-212.
32. Shaffer KA, Jones TA, Canelas DA, DeSimone JM. Dispersion polymerizations in carbon dioxide using siloxane-based stabilizers. *Macromolecules.* 1996;29:2704-2706.
33. Canelas DA, Betts DE, DeSimone JM. Poly(vinyl acetate) and poly(vinyl acetate-*co*-ethylene) latexes via dispersion polymerizations in carbon dioxide. *Macromolecules.* 1998;31:6794-6805.
34. Yates MZ, Li G, Shim JJ, Maniar S, Johnston KP, Lim KT, Webber S. Ambidextrous surfactants for water-dispersible polymer powders from dispersion polymerization in supercritical CO_2. *Macromolecules.* 1999;32:1018-1026.
35. Shiho H, DeSimone JM. Dispersion polymerization of acrylonitrile in supercritical carbon dioxide. *Macromolecules.* 2000;33:1565-1569.
36. Liu H, Yates MZ. Development of a carbon dioxide-based microencapsulation technique for aqueous and ethanol-based latexes. *Langmuir*. 2002;18:6066-6070.
37. Mawson S, Yates MZ, O'Neill ML, Johnston KP. Stabilized polymer microparticles by precipitation with a compressed fluid antisolvent. 2. Poly(propylene oxide)- and poly(butylene oxide)-based copolymers. *Langmuir.* 1997;13:1519-1528.

Manuscript received Dec. 19, 2003, and revision received Jun. 18, 2004.